

Effect of Silk Fiber to the Mechanical and Thermal Properties of Its Biodegradable Composites

Mei-Po Ho,¹ Hao Wang,¹ Kin-Tak Lau,^{1,2} Jinsong Leng³

¹Centre of Excellence in Engineered Fiber Composites, Faculty of Engineering and Surveying, University of Southern Queensland, Toowoomba, Queensland, Australia

²Department of Mechanical Engineering, The Hong Kong Polytechnic University, Kowloon, Hong Kong, SAR, China

³Center for Smart Materials and Structures, School of Aeronautics, Harbin Institute of Technology, China

Correspondence to: K.-T. Lau (E-mail: Lau@usq.edu.au or mmktlau@polyu.edu.hk)

ABSTRACT: In recent years, natural fiber-reinforced biodegradable thermoplastics are being recognized as an emerging new environmentally friendly material for industrial, commercial, and biomedical applications. Among different types of natural fibers, silk fiber is a common type of animal-based fiber, has been used for biomedical engineering and surgical operation applications for many years because of its biocompatible and bioresorbable properties. On the basis of our previous study, a novel biodegradable biocomposite for biomedical applications was developed by mixing chopped silk fiber and polylactic acid (PLA) through the injection molding process. This article is aimed at studying the dynamic mechanical and thermal properties of the composite in relation to its biodegradation effect. At the beginning, it was found that the initial storage modulus of a silk fiber/PLA composite increased while its glass transition temperature decreased as compared with a pristine PLA sample. Besides, the coefficient of linear thermal expansions (CLTE) of the composite was reduced by 28%. This phenomenon was attributed to the fiber–matrix interaction that restricted the mobility of polymer chains adhered to the fiber surface, and consequently reduced the T_g and CLTE. It was found that the degraded composite exhibited lower initial storage modulus, loss modulus and $\tan \delta$ ($\tan \delta$) but the T_g was higher than the silk fiber/PLA composite. This result was mainly due to the increase of crystallinity of the composite during its degradation process. © 2012 Wiley Periodicals, Inc. *J. Appl. Polym. Sci.* 000: 000–000, 2012

KEYWORDS: composites; fibers; thermodynamics

Received 30 October 2011; accepted 21 February 2012; published online

DOI: 10.1002/app.37539

INTRODUCTION

There is no doubt that biodegradable polymer composites (commonly called “biocomposites”) are generally recognized as one of the key materials in coming centuries. By constituting naturally degradable fiber (such as nature fiber and synthesized biopolymer-based fiber) and biodegradable polymer matrix (such as PLA, PBS, PCL, etc.), manufactured by various traditional or specific processes to form the biocomposites, their properties can be tailor-made to satisfy various product requirements without additionally inducing any harmful effect to the environment. In biomedical engineering applications, biocomposites can be used to produce artificial joints and tissues implanting into the human body.¹ In the implantation, traditional metallic materials possess many inherent problems that may cause either an infection induced inside the human body or an undesirable/unexpected result achieved.² For an example, by using steel as a bone fixator, it is too stiff and leads to that a

stress-shielded bone delays bridging and then an incompletely healed bone is resulted after the removal of the fixator. This weakened bone also suffers serious bone loss (osteoporosis) including intracortical porosity, cortical thinning, and correspondingly greater loss of mechanical properties.³ Besides, the need of the second surgery for removing the fixator, corrosion of the fixator inside the human body, and bone atrophy associated with rigid metallic fixation devices increase the probability of bone infection.⁴ Moreover, the postoperative radiotherapy as well as X-ray for diagnostic imaging on healing bones is interfered by the fixator too.⁵

To overcome aforementioned problems of using metallic materials for bone fixators, silkworm silk fiber reinforced polymer composites, based on their inherent mechanical, biocompatible and bioresorbable properties have been found as a desirable biocomposite for this application. Silk fiber as sutures for human wound dressing have been used for centuries.⁶ Regenerated silk

© 2012 Wiley Periodicals, Inc.

solutions have been used to form a variety of biomaterials, such as gels, sponges, and films, for medical applications.⁷ Silk has been exploited as a scaffold biomaterial for cell culture and tissue engineering *in vitro* and *in vivo*.⁸ However, before adopting this new class of biocomposite into real-life applications, study, and clarification on the correlations between its thermal, mechanical, and degradation properties are necessary for the long term prediction of its performance in human body. As this composite is designed for bone fixators, it has to be in a functional condition at the temperature below its glass transition temperature (T_g) in order to assure that the mechanical performance is adequate at all the time the composite inserted inside the human body. Creeping (dead load of fractured sections), fatigue (repeated bending), and degradation (bioresorption) are also other key factors that may affect the performance of the composite with time. The fixators should also possess moderate stiffness and good damping properties to absorb external impact and vibration load to protect a fractured bone. Therefore, the storage modulus and loss energy of a composite fixator should be high enough to enhance their ability to absorb and dissipate energy, respectively within the predetermined period, i.e., during an acceptable duration when the fixator is in the process of degrading. In view of this, thermo-mechanical and dynamic mechanical analyses, and density measurement are investigated in this article.

Thermo-Mechanical Properties

The viscoelastic behavior of polymer during their deformation and flowing process is mainly dependent on the temperature and time (frequency). Molecular rearrangement happens during the process can minimize the formation of localized stresses. Polymer's molecules would store a portion of applied energy and dissipate the rest to other dissipative processes such as the formation of cracks, heat, sound, and vibration motion) under a repeated loading condition. The characteristic parameter that is used to represent the viscoelasticity of polymer is “ $\tan \delta$.”⁹ This parameter is a function of temperature and its relationship with the storage modulus (E') and loss modulus (E'') is:

$$\tan \delta = E''/E'$$

Dynamic mechanical analysis (DMA) allows for a quick and convenient measurement of material properties in which a sample is under an oscillating force and, the material's deformation parameters including modulus and damping are measured as a function of temperature, frequency, or time, or combination thereof. The test fixtures depend on the samples, desired loading and result, used for various property characterizations. DMA provides material properties including storage modulus (E'), loss modulus (E'') and relaxation processes in polymers, specially the glass transition (T_g). The storage and loss moduli are proportional to the energy stored and dissipated, respectively per cycle. The E' characterizes the elastic behavior of the material, and the E'' characterized the viscous behavior. The ratio of energy dissipated to energy stored is the tangent of the phase angle called $\tan \delta$. Compared with Differential Scanning Calorimetry (DSC), weak glass transitions can be easily and precisely determined by DMA due to its approximately one decade higher sensitivity to glass transitions.¹⁰

MATERIAL PREPARATION AND EXPERIMENTS

Injection Molding

The biodegradable polymer-PLA as matrix, for this study is a neat grade commercial type (the brand name of NatureWorks PLA Polymer). Silkworm silk fiber (hereafter called “the silk fiber”) with the average fiber diameter of 100 μm was supplied by Ocean Verve, Hong Kong. The inherent body structure of silk fiber is composed of two cores of fibroin which exists in a paired of organ. The fibroin itself is a bundle of several fibrils and each fibril contains many microfibrils. Therefore, due to the microfibrils are of a very small in diameter and close packed, wettability is always an issue to ensure good bonding between the silk fiber and matrix in a silk fiber polymer composite. Besides, a sericin layer also plays a critical role as it may isolate the physical contact or direct chemical bonding between the fiber and matrix. This layer is mainly made by protein as a coating and adhesive of the silk fiber. As mentioned in a previous literature, this layer would affect the bonding between the fiber and polymer-based matrix, and thus worsen the mechanical properties of silk fiber composites.¹¹ In this study, the silk fiber received was in a sericin free status (commonly called “degummed silk fiber”).

Silk fiber/PLA composite samples were made by using the Hakke MiniLab twin-screw micro-extruder. Before mixing the silk fiber with PLA, all silk fibers were chopped into 5 mm in length in order to avoid coiling with the screws and fiber stretching plastically either co- or counter rotating during the injection process. These fibers were dried up inside an oven to remove excessive moisture before the injection molding process. On the basis of our preliminary study, the optimal fiber content, in terms of the moldability inside the PLA environment was 5 wt %. A uniform temperature of 180°C was maintained at all zones inside in the process. The mixture of the silk fibers and molten PLA were then transferred to the Thermo Hakke small scale injection molding machine. The injection cylinder and the mould were preheated to desirable temperatures of 200 and 45°C, respectively, the composite samples were made in a dumbbell shape according to ASTM D3039.

Degradation

In terms of *in vitro* biodegradation test, PLA and composite samples were placed into separated tanks containing Phosphate Buffered Saline (PBS) solution. White dry powder of PBS was diluted with 1 L of deionized water (DI) with ultimately the pH level of 7.4 being achieved. Two types of samples were stored into the tanks with 500 mL of solution each. The tanks were then stored in a humidified, thermostable, and orbital-shaking incubator at 37°C with 100 rpm for 1 year. The PBS solution was changed every month in order to maintain the pH level inside the tanks.

Density Measurement

The density of the fibers was determined by pycnometry. The density is simply defined as mass divided by volume (g/cm^3). Water was used as reference liquid at 23°C.

Thermomechanical Analysis

The thermal expansion of a material is the changes in length or volume due to the changes in moisture content, curing, release

of stresses, phase changes, etc. under heating. It is an important data for manufacturing and functioning of biodegradable and bioresorbable composite bone fixators. TMA was conducted by a PerkinElmer TMA 7 instrument. The processing temperature for the TMA experiments according to the ASTM standard D 696 was controlled from 40 to 165 °C at a scan rate 10 °C/min with a penetration probe 1.0 mm in diameter under a uniaxial stress of 0.12 MPa. The change in length for testing specimens over a corresponding change in temperature was recorded.

Dynamic Mechanical Analysis

DMA was processed according to the international standard D 5023-07. All samples were investigated under a flexure test by TA Instrument DMA Q800 with a multifrequency-strain mode. Four different types of samples with the dimension of 60 mm × 5 mm × 1.5 mm were tested, these samples were (i) pure PLA, (ii) degraded PLA, (iii) silk fiber/PLA composite, and (iv) degraded silk fiber/PLA composite. Pure polymer is a control to compare the results with remaining samples. The degraded PLA and degraded composite were prepared as specified in previous section. The actual dimensions of each sample were measured afterward. The samples were then gripped horizontally by dual cantilever. The linear displacement amplitude was set to 15 μm. Thermal scans were conducted from 20 to 150 °C at a ramping of 3 °C/min with soak time 2 min for step increases.

RESULTS AND DISCUSSION

Density Measurement and TMA

Table I summarizes the results from the density and TMA measurements. The results show that the density of the composite sample decreases by 1.6% as compared with the pure PLA. It is a reasonable finding as the density of the silk fiber is lower than that of the PLA. On the basis of the principle of the “Rule of Mixture,” the density of the composite is lower depending on the amount of silk fiber to be added. Moisture content in the silk fiber is also an affecting factor as voids may be formed during the molding process. Entrapment of air within the space between fibrils may also be an issue. In reality, light weight and controllable porosity are desirable parameters for composite bone fixators as it can reduce their deadweight and control the rate of bioresorption inside the human body.¹²

TMA is used to measure variations in dimensions of a sample (length or volume), which is subjected to a nonoscillatory loading. Therefore, TMA is commonly used to determine the thermal expansion nowadays.¹³ The mean coefficient of linear thermal expansion (CLTE) obtained from TMA measurement is used to reflect the dimensional changes as well as thermal stresses caused by the thermal variation.¹⁴ The coefficient of lin-

ear thermal expansion for the desired temperature range can be calculated according to the following equation:¹³

$$(\alpha) = (\Delta L)/(L)(\Delta T) \quad (1)$$

where

- α = Mean coefficient of linear thermal expansion for the reference material at the midpoint of the ΔT range, in °C⁻¹,
- L = Length of the sample at room temperature, in μm,
- ΔL = Change in length of the reference material due to heating, in μm,
- ΔT = Temperature difference over which the change in specimen length is measured, in °C.

Based on the results shown in Table I, the coefficient of linear thermal expansions (CLTE) of the composite decreases by 28%. The results exhibit the improvement of physicomechanical properties in the composite as compared with the pure PLA. In general, CLTE of a fiber reinforced polymer composite is lower than that of its pure matrix system (i.e., PLA in this case) due to the low CLTE of the fiber. In the real practice, low CLTE of the composite is desirable for all engineering applications to minimize any thermo-dimensional change of structures during manufacturing process (which may cause the generation of residual stress after curing) and in use.¹⁵ Therefore, the lower the value of CLTE measured, the better the property for a bone fixator to be achieved.¹⁶

Krevelen and Volemetric¹⁶ suggested that the molar thermal expansibility of a polymer is related to the van der Waals volume of repeated units of a polymer. Moreover, Bondi¹⁷ has defined that the van der Waals volume as volume occupied by a molecule, which is impenetrable by the other molecules having thermal energy at ordinary temperature. As silk fiber is a macro-sized natural fiber, it cannot penetrate into such a small volume of the polymer and cause the decrement in thermal expansion of the composite. Therefore, the thermal expansion of composite is mainly affected by the interaction between the fiber and the PLA (matrix). This interaction may restrict the mobility of polymer chains which adheres on the fiber surface and thus, cause the reduction in the thermal expansion of the composite.¹⁸ The improvement of thermo-mechanical stability and dimensional stability of biocomposites by using natural fiber has been addressed by Lee et al.¹⁹ In their study, poly(butylene succinate) (PBS) was used as a base polymer reinforced by silk fiber.

Dynamic Mechanical Properties

As the low storage modulus, it demonstrates the ease of deformation of a material by an applied load. Contrarily, high storage modulus is more desirable as it represents high stiffness and load bearing of the material at a specified temperature range. Figure 1(a–c) show the storages modulus (E'), loss modulus (E''), and $\tan \delta$ of the pure PLA and the composite as a function of temperature, respectively. Table II is the summary of the DMA results.²⁰

In Figure 1(a), the storage modulus of the composite is higher than that of the pure PLA. It may be due to the existence of

Table I. The Density Measurement and the TMA Results of the Pure PLA and the Silk Fiber/PLA Composites

	Density (g/cm ³)	ΔL (μm)	α (μm m ⁻¹ °C ⁻¹)
Pure PLA	1.26	46.032	227.875
Composite	1.24	32.748	164.223
Change of percentage (%)	-1.6	-29	-28

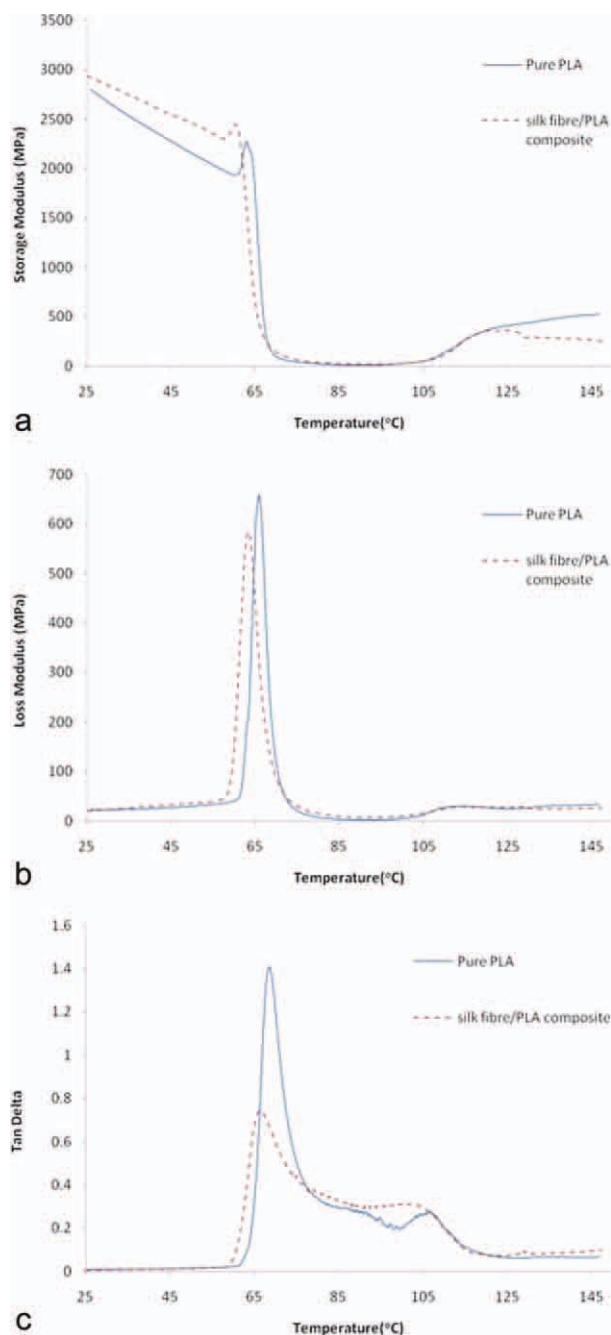


Figure 1. (a) Storage modulus (b) Loss modulus and (c) $\tan \delta$ versus temperature of the pure PLA compare with the composite. [Color figure can be viewed in the online issue, which is available at wileyonlinelibrary.com.]

silk fiber which formed as physical cross linkage and allowed stress transfer between the silk fiber and the PLA.^{21,22} The mobility of PLA macromolecules was therefore counteracted by the silk fibers because of the difference glass transition temperatures (T_g s) between two materials. Consequently, the stiffness of the composite was increased.^{21–23} The PLA sample which incorporated with silk fiber revealed higher damping capabilities. This behavior could be related to the interfacial condition of the

composite. Partial energy lost in the interface between the PLA and the silk fiber which is due to macroscopic frictional effects in this heterogeneous system.²⁴

The figure shows the variation of storage modulus of the composite versus the change of temperature. At the beginning of the experiment, the macromolecules of the composite are comparatively highly immobile and exist in a close and tight packing form and thus, resulting in high storage modulus. As temperature increases the macromolecules become more mobile and lose their close packing arrangement. As a result the storage modulus of the composites decreases.¹⁵ Therefore, it is obviously observed that the E' decreases gradually starting from an ambient temperature and then dramatically after 60°C. The reduction in the E' with an increase of the temperature is associated with softening of the matrix at higher temperature.

As PLA is a bulk polymer which has no high-strength characteristics, it is easy for plastic deformation during application. The loads generated through patient's movements or external forces which are suffered from the patient daily are transferred to the fixator. The pure PLA bone fixator would be deformed after applying loads on it. To make matters worse, the deformed PLA bone fixator cannot protect and hold the broken bones properly afterward, the bone would be refracture again. Hence, forces which are transferred to the bone fixator must be dissipated over a large area to prevent the bone fixator from failing. From the results obtained, Silk fiber/PLA composite samples exhibited higher stiffness and thus the forces could be dissipated over a larger extent.

The E'' in viscoelastic solids measures the energy dissipated as heat representing the viscous portion. Comparing the curves of E'' of the two different samples as shown in Figure 1(b), T_g is measured at a peak of the curves. The peak of the composite is slightly shifted down to a lower temperature as compared with the PLA with a narrow range at the transition region. This effect is exemplified through the broader slope of the transition region from the curves in Figure 1(a) and accompanied by peak widening from the loss modulus curves. The changes of the T_g between pure PLA and the composite are dependent on the fiber length, fiber content and their interfacial bonding properties. Besides, only amorphous phase of partial crystalline PLA is involved in affecting the condition of T_g , the mobility of the PLA is counteracted by the fibers.¹⁰

$\tan \delta$ is the ratio of the E''/E' or, explicitly is the ratio of energy lost to energy retained in the loading cycle. High value of $\tan \delta$ means that once the deformation is induced, the material will not recover to its original status. The first peak at the $\tan \delta$ curve indicates a relaxation process while the second peak represents the T_g where molecules regain their mobility. It is found in Figure 1(c) that there is no substantial difference in $\tan \delta$ for both the composite and PLA at 37°C, a simulated human body temperature. However, a significant decrement of the height and the sharpness of the peak are obtained as shown in the figure as the increase of content of silk fiber in PLA.²⁵ Such phenomena are coincident with other literatures for fiber-reinforced thermoplastics.²⁶ Pure PLA shows a sharp and intense peak because there is no restriction to the chain motion, where

Table II. DMA Data of Compression-Molded Composites in Terms of the Mean Storage Modulus (E'), at 25 and 37°C, and Glass Transition Temperature (T_g) as Defined by Peaks in Loss Modulus and $\tan \delta$

Material	Storage modulus		Loss modulus		Tan δ	
	At 25°C	At 37°C	T_g (°C)	At 37°C	T_g (°C)	At 37°C
Pure PLA	2.795	2.478	65.91	24.680	68.58	0.010
Composite	2.940	2.697	63.28	26.769	66.13	0.008
Degraded PLA	2.772	2.439	67.75	25.7414	70.07	0.011
Degraded composite	2.053	1.956	64.04	264.013	69.28	0.135

the composite hinders the chain mobility and results in the reduction of the sharpness and height of the $\tan \delta$ peak.

As damping in the transition region implies the imperfection of a material in its elastic phase, and some of the energy is used to deform it during DMA and also directly dissipate into heat. Thus, the mechanical loss that overcame the friction of intermolecular chains was reduced in the composite. This result indicates that the silk fiber can be used to restrict the mobility of the composite so as their E' was higher than that of the pure PLA.⁶ The reduction in $\tan \delta$ also denotes an improvement in the hysteresis of the system and a reduction in the internal friction.⁷ Moreover, for the PLA reinforced by the silk fiber, the area under the $\tan \delta$ curve is smaller than that the curve measured by the pure PLA. Since the PLA content is decreased to the same extent and only the amorphous phase of the partial crystalline polymer is involved in the glass transition.^{6,27}

DMA on Degraded Pure PLA and Silk Fiber Reinforced Composites

Figures 2 and 3 show the dynamic mechanical properties, as a function of temperature of the pure PLA and the composite as compared with their degraded statuses, respectively. As shown in Figure 2(a), the pure PLA and degraded PLA exhibit similar initial E' . As shown in Table II, the E' of the degraded composite is the lowest among all other samples. Comparing with degraded PLA with the pure PLA, it can be proved that the E' of the pure PLA decreases because of the degradation process. Same as PGA PLGA and PCL, PLA processes the bulk erosion after absorbing the moisture. The difference to the surface erosion, bulk erosion would be taken place throughout all degraded samples. Ingress of water is normally faster than that the rate of degradation. Therefore, the weight of the samples increases at the beginning of the degradation process and their volumes were then increased subsequently.¹¹

In Table II, it is found that the E' of degraded composite is much lower than that of the degraded PLA. The decrement in the E' is mainly caused by the water absorption of silk fiber in the composite. Silk proteins are stored in the silk gland and transported down the spinning duct in a lyotropic liquid crystalline state in silkworm silk glands. To produce this state, the protein molecules of the silk fiber must be amphiphilic, which is having a combination of hydrophobic and hydrophilic blocks or groups.²⁸ The hydrophilic character of natural fiber is responsible for the water absorption in the composites, and therefore increasing the amount of fiber would cause more water to be absorbed.²⁹ As the water absorbability of the silk

fiber is higher than the PLA, it would accelerate the degradation process of the degraded composite. It further proves that the hydrophilic effect of the silk fiber does affect the water absorbability in its related composites.¹¹

Figure 3(a) shows that there is a difference in a large extent of E' between the composite and the degraded composite. It is also demonstrated that within the range of 61 and 68°C, the values of E' for all samples decrease rapidly. This implies that the contribution of fiber stiffness to the modulus of PLA is minimal at its glassy zone.³⁰ Besides, Figure 3(a) shows a slight broadening of the loss modulus peak of degraded PLA compared with degraded silk fiber reinforced composite. This could be due to the increase in energy dissipation caused by the addition of silk fibers which increase the degradation process. Tsukada et al.¹ have found that the shrinkage of silk fiber is about 1.3% because of the loss of moisture during heating. As the shrinkage of the silk fiber is different to the PLA, the deterioration of the interfacial adhesion and bond strength between the PLA and silk fiber were found which induces the dramatically drop of the initial E' of silk fiber/polymer composites. Therefore, the combined effect of the silk fiber shrinkage, and the mismatch of thermal expansions between the silk fiber and the PLA resulted in weakening the properties of the degraded composite.⁷

The reduction of E' of the degraded composite compared with the composite was due to the damage of matrix, deteriorated interfacial adhesion and poor bonding strength between the silk fiber and the matrix.³¹ The deteriorated interface adhesion is susceptible to the degradation because of excessive interface reactions which would speed up the hydrolysis of the degraded composite. As a result, the interface could no longer be able to provide a full stress transfer from the matrix to the fiber effectively, and thus the E' modulus of the degraded composite decreased.

Chemical combinations between the polymer chains, Van der Waals interaction, and the hydrogen bonding in the molecular construction are responsible for the ability of the polymer to bear externally applied stresses. Moreover, the strength of the interface between fiber and matrix has the significance effect on E' . The degradation process starts with the swelling of silk fibers because of the water penetrating into the interface that develops stress at the interface and causes micro-cracking of the matrix around the swollen fibers. The cracks also accelerate the water absorption and its attack on the interface through capillarity mechanism. The residues of the degraded substances start leaching from the fibers. These eventually lead to the ultimate

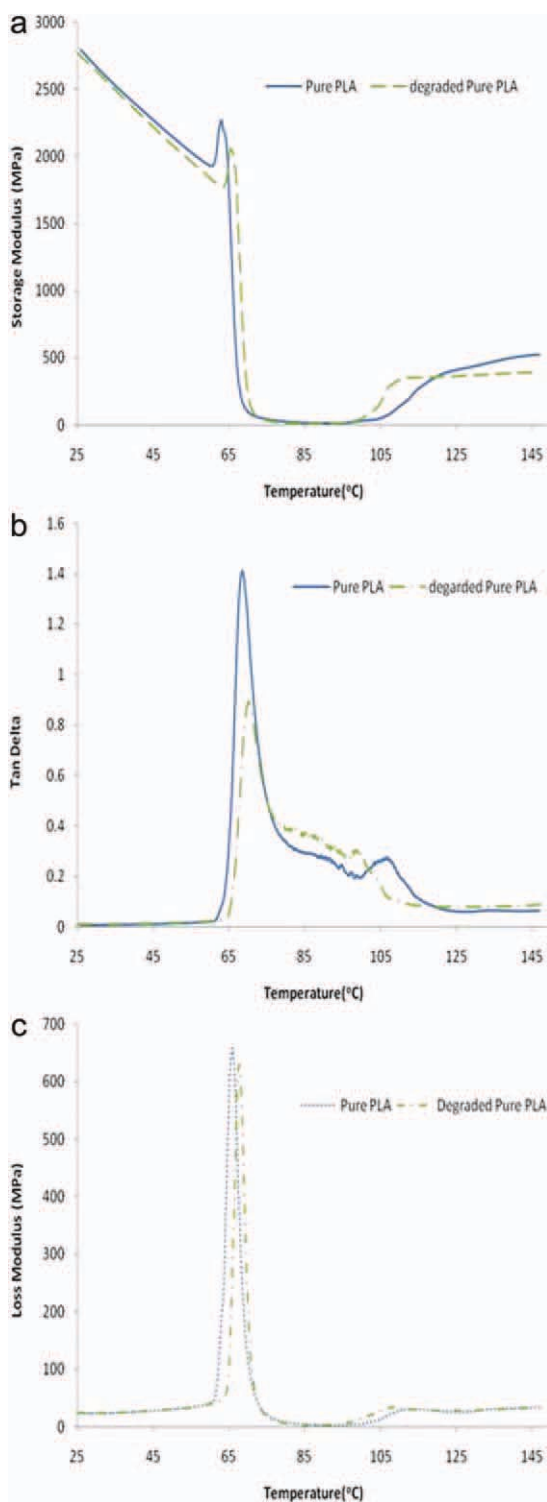


Figure 2. (a) Storage modulus (b) Loss modulus and (c) $\tan \delta$ versus temperature of the pure PLA compared with the degraded PLA. [Color figure can be viewed in the online issue, which is available at wileyonlinelibrary.com.]

debonding between the fiber and the matrix^{32,33} (Figure 4). Therefore, the voids in the composite increase and these voids also increase the surface area and thus speed up the degradation

process for intra- and intermolecules bonding breakage. Therefore, the macromolecules are loose packed and not restricted. Because of the increased mobility of polymer molecules in the degraded composite with poor adhesion, E' of degraded

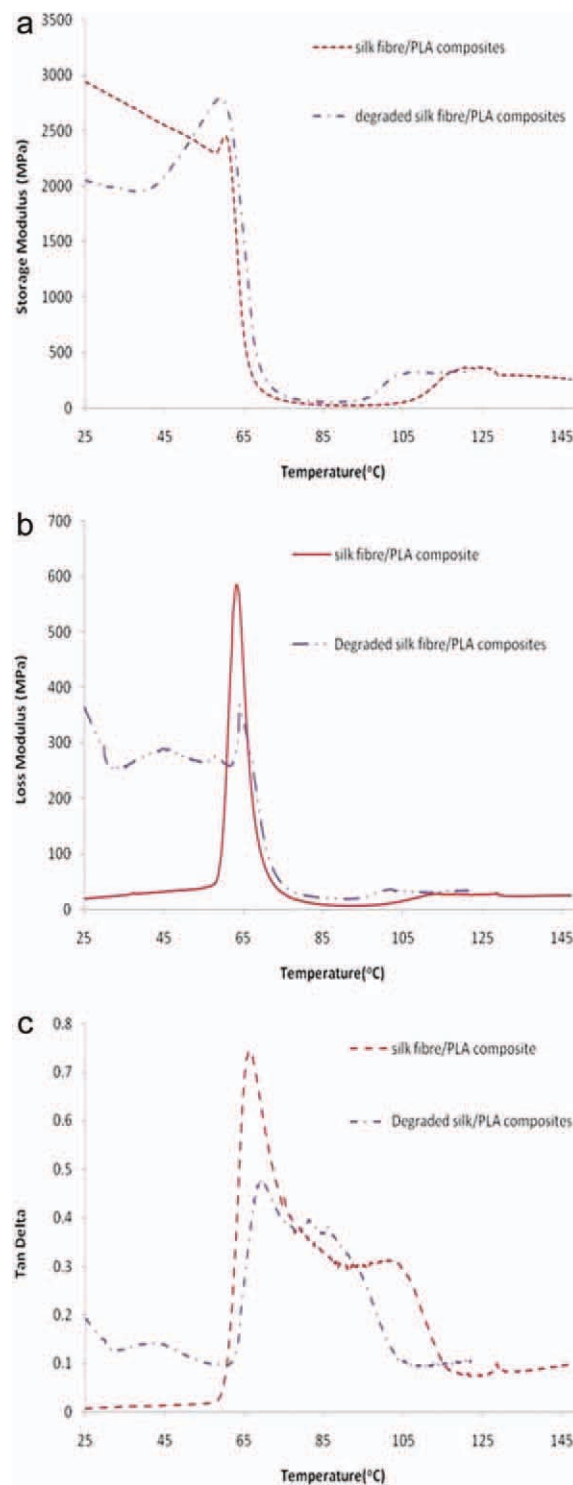


Figure 3. (a) Storage modulus (b) Loss modulus and (c) $\tan \delta$ versus temperature of the composite compared with the degraded composite. [Color figure can be viewed in the online issue, which is available at wileyonlinelibrary.com.]

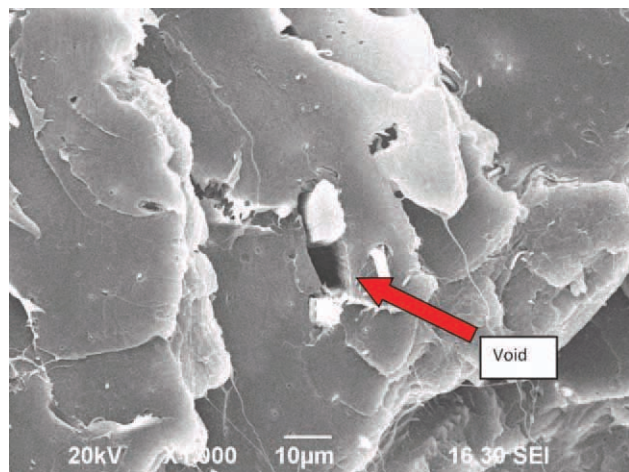


Figure 4. The void formed because of the debonding. [Color figure can be viewed in the online issue, which is available at wileyonlinelibrary.com.]

composite was therefore lower than that of the composite with better bonding interface. Nevertheless, the bonding between the silk fiber and PLA could be damaged easier than the internal bonding in the pure PLA because of the opposite nature of hydrophobicity as silk fiber is amphiphilic. Besides, When samples were immersed into the PBS solution, water molecules penetrated into the PLA, the hydrolysis and plasticization of the PLA would damage the chemical bonding, in the case of experiencing a stress, greater strain may be induced, which would lead to a decrease of the E' .²² On the other hand, the viscous nature of water may interfere itself on the overall viscoelastic of the system.²⁴

Comparing the E'' and $\tan \delta$ of the pure PLA with the degraded PLA, and the composite and the degraded composite, respectively as shown in Figures 2(b,c) and 3(b,c), the T_g of degraded samples were higher than that of nondegraded samples. The glass transition can be thought as the softening point of amorphous regions of polymers. The result shown in the figures are mainly because of the water which acted as a plasticizer and the increase of the crystallinity of the degraded samples. Although the degradation process increased the crystallinity of the PLA through plasticization by water, certain regions in the PLA were hydrolyzed by bulk erosion.^{34,35} Therefore, it can be explained that even the crystallinity of the degraded samples increased, the modulus of the sample decreased. As the debonding of the interface caused by the distinct moisture, expanding coefficient between the fiber and matrix in the plasticization process, it would also be a factor to lower the $\tan \delta$.³¹ Therefore, the T_g obtained from both E'' and $\tan \delta$ increased because of the increment of the mobility.

Through the degradation process, the porosity of the degraded composite and the degraded PLA increased which also increased their damping effect. Hence, a relatively less energy was used to overcome the frictional forces between molecular chains so as to decrease mechanical loss. The energy absorbing process of the degraded composite was smaller because the presence of the silk fiber in the degraded composite after the degradation process.⁹

CONCLUSIONS

The dynamic mechanical and thermal properties of PLA, degraded PLA, silk fiber/PLA composite, and degraded silk fiber/PLA composite samples in relation to their biodegradation effect were studied. At the beginning, it was found that the initial storage modulus of the silk fiber/PLA composite increased while its glass transition temperature decreased as compared with the PLA sample. Moreover, the coefficient of linear thermal expansions (CLTE) of the silk fiber/PLA composite was reduced by 28%. This phenomenon was attributed to the fiber–matrix interaction that restricted the mobility of polymer chains adhered to the fiber surface, and consequent reduced the T_g and CLTE. As compared with the degraded silk fiber/PLA composite, it was found that the degraded composite exhibited lower initial storage modulus, loss modulus and $\tan \delta$ but higher T_g than the silk fiber/PLA composite. This result was mainly due to the increase of crystallinity of the composite during its degradation process.

ACKNOWLEDGMENTS

This project is supported by The Hong Kong Polytechnic University Grant (G-U688) and the University of Southern Queensland.

REFERENCES

1. Tsukada, M.; Gotoh, Y.; Yasui, H. *J. Seric. Sci. Jpn.* **1995**, *64*, 435.
2. Thakur, A. J. *The Elements of Fracture Fixation*; Churchill Livingstone: University of Michigan, USA, **1997**.
3. Flahiff, C. M.; Blackwell, A. S.; Hollis, J. M. *J. Biomed. Mater. Res.* **1996**, *32*, 419.
4. Burns, A. E.; Varin, J. *J. Foot. Ankle. Surg.* **1998**, *37*, 37.
5. Tams, J.; Rozema, F. R. *Int. J. Oral Maxillofac. Surg.* **1996**, *25*, 20.
6. Wanjun, L.; Manjusri, M.; Per, A.; Lawrence, T. D.; Amar, K. M. *Polymer* **2005**, *46*, 2710.
7. Huda, M. S.; Mohanty, A. K.; Drzal, L. T.; Schut, E.; Misra, M. *J. Mater. Sci.* **2005**, *40*, 4221.
8. Akbar, A. K.; Mai, Y. W. *Compos. A* **2002**, *33*, 1585.
9. Faughnan, P.; Bryan, C. *J. Mater. Sci. Lett.* **1998**, *17*, 1743.
10. Ho, M. P.; Lau, K. T.; Wang, H.; Bhattacharyya, D. *Compos. B* **2011**, *42*, 117.
11. Wielage, B.; Lampke, T.; Utschick, H.; Soergel, F. *J. Mater. Proc. Technol.* **2003**, *139*, 140.
12. Shamsul, J. B.; Nurhidayah, A. Z.; Ruzaidi, C. M. *J. Appl. Sci. Res.* **2007**, *3*, 1544.
13. Kaeagiannidis, G. P.; Stergiou, A. C.; Karayannidis, G. P. *Eur. Polym. J.* **2008**, *44*, 1475.
14. Van Krevelen, D. W. In *Properties of Polymers: Their Estimation and Correlation with Chemical Structure*; Elsevier: Amsterdam, Oxford, New York, **1976**; Chapter 4, p 67.

15. Huda, M. S.; Drzal, L. T.; Misra, M. *Ind. Eng. Chem. Res.* **2005**, *44*, 5593.
16. Yang, H. S.; Wolcott, M. P.; Kim, H. S.; Kim, H. J. *J. Therm. Anal. Calorim.* **2005**, *82*, 157.
17. Andrzej, K. B.; Adam, J.; Dietrich, S. *Compos. A* **2009**, *40*, 404.
18. Huang, G. *Mater. Des.* **2009**, *30*, 2774.
19. Bondi, A. *J. Phys. Chem.* **1964**, *68*, 441.
20. Idicula, M.; Malhotra, S. K.; Joseph, K.; Thomas, S. *Compos. Sci. Technol.* **2005**, *65*, 1077.
21. Rana, A. K.; Mitra, B. C.; Banerjee, A. N. *J. Appl. Polym. Sci.* **1999**, *71*, 531.
22. Hedenberg, P.; Gatenholm, P. *J. Appl. Polym. Sci.* **1995**, *56*, 641.
23. Averous, L.; Boquillon, N. *Carbohydr. Polym.* **2004**, *56*, 111.
24. Mano, J. F.; Reis, R. L. *Mater. Sci. Eng.* **2004**, *370*, 321.
25. Reading, M.; Haines, P. J. *Thermal Methods of Analysis*; London: Chapman & Hall, **1995**; Chapter 4.
26. Lee, S. M.; Cho, D.; Park, W. H.; Lee, S. G. *Compos. Sci. Technol.* **2005**, *65*, 647.
27. Huda, M. S.; Drzal, L. T.; Mohanty, A. K.; Misra, M. *Compos. Sci. Technol.* **2006**, *66*, 1813.
28. Jacob, M.; Francis, B.; Thomas, S.; Varughese, K. T. *Polym. Compos.* **2006**, *1*, 671.
29. Bini, E.; Knight, D. P.; Kaplan, D. L. *J. Mol. Biol.* **2004**, *335*, 27.
30. Espert, A.; Vilaplana, F.; Karlsson, S. *Compos. Part A* **2004**, *35*, 1267.
31. Wielage, B.; Lampke, T. H. *J. Mater. Proc. Technol.* **2003**, *139*, 140.
32. Athijayamania, A.; Thiruchitrambalamb, M.; Natarajana, U.; Pazhanivel, B. *Mater. Sci. Eng. A* **2009**, *517*, 344.
33. Chen, H.; Miao, M.; Ding, X. *Compos. A* **2009**, *40*, 2013.
34. Cai, H.; Dave, V.; Cross, R. A.; McCarthy, S. P. *J. Polym. Sci. Part B: Polym. Phys.* **1996**, *34*, 2701.
35. Gonzalez, M. E.; Ruseckaite, R. A.; Cuadrado, T. R. *J. Appl. Polym. Sci.* **1999**, *71*, 1223.